NUMERICAL SIMULATION STUDY ON FLEXURAL BEHAVIOUR OF RC BEAMS STRENGTHENED WITH ECC LAYER AND CFRP SHEETS

Nguyen Cong Luyen*, Mai Anh Duc, Nguyen Ngoc Han, Hoang Duc Nhan, Huynh Trieu

The University of Danang - University of Science and Technology, Danang, Vietnam

*Corresponding author: ncluyen@dut.udn.vn

(Received: April 14, 2025; Revised: May 10, 2025; Accepted: May 19, 2025)

DOI: 10.31130/ud-jst.2025.23(6A).209E

Abstract - This study presents a numerical study on the structural behavior of reinforced concrete (RC) beams strengthened with Engineered cementitious composites (ECC) layer and Carbon Fiber Reinforced Polymer (CFRP) sheets. The numerical model was developed using ABAQUS/CAE three-dimensional finite element (FE) model package, in which material nonlinearities were considered. By comparing with experimental results reported in the literature, it was shown that the numerical modelling findings agreed well with test data not only in terms of failure mode but also flexural strength capacity. The average deviation between the experimental and modelling results in terms of flexural strength of strengthened RC beams is only 4.4%. This demonstrates that the developed FE model can be a powerful tool in the assessment of the strengthening efficiency of RC beams strengthened with ECC layer and CFRP sheets.

Key words - Engineered Cementitious Composite (ECC); CFRP sheet; strengthened RC beam; flexural behavior; finite element modelling

1. Introduction

Reinforced concrete (RC) beams are usually used in civil engineering structures (e.g., bridges, buildings, etc.) but they are often subjected to deterioration due to aging, environmental conditions, and increased service loads [1]. Thus, there is a need to enhance the load-bearing capacity and lengthen the service life of the RC beams. Various strengthening methods have been employed in RC beams [2-5]. Among those, using carbon fiber reinforced polymer (CFRP) seems to be an appropriate solution due to its high strength and ease of installation. However, applying CFRP directly to the concrete surface of RC beams results in an unexpected drawback. When the RC beam is subjected to a sagging moment, due to a low tensile strain capacity of concrete, flexural cracks and stress concentration appear in the interfacial surface between concrete and CFRP, leading to the debonding of the CFRP sheet and thus compromising its strengthening capacity [6-8]. Engineered Cementitious Composites (ECC), which exhibits excellent characteristics in tension such as high tensile strain capacity, ability to develop multiple tiny cracks, crack bridging effects, and so on, could be a suitable candidate for combining with CFRP to be an effective strengthening system applying in RC beams [9-10].

Substantial studies on hybrid systems of ECC layer and CFRP sheet in strengthening RC beams have found that using this system could improve the load-carrying capacity of the beams [11-14]. For instance, Wu et al. [11] conducted an experimental study to investigate the flexural strength of CFRP-ECC-strengthened concrete beams. The results found the premature debonding at the interface between strengthening materials and the bending capacity of the strengthening concrete beam was improved. A similar finding was reported in an experimental investigation conducted by Zhou et al [12] on externally bonded FRP beams. Hu et al. [13] experimentally and theoretically studied the flexural behaviour of corroded RC beams retrofitted by an ECC-CFRP hybrid system. The results indicated that the retrofitting system could recover the flexural strength of the corroded beam to a value close to that of the virgin beam. Moreover, the experimental study of Zhang et al. [14] on the effect of strengthening system of ECC material and CFRP sheets on the flexural behavior of RC beams shows that a significant improvement can be recorded if this hybrid system is used to retrofit the beam, not only in terms of flexural strength but also cracking and yield strength. Using the ECC layer could delay the debonding of CFRP from concrete surfaces [14]. A research gap found in these studies is that there are virtually no numerical models reported to simulate the behaviour of ECC-CFRP strengthening RC beams. In addition, a limitation of the aforementioned studies is that the effects of different parameters have not been adequately investigated due to the restriction in time and resources. A more effective approach in investigating this strengthening system in RC beams, thus, should be prioritized. In this paper, the authors employ the finite element analysis ABAQUS tool to simulate the hybrid strengthening system of ECC material and CFRP sheets applied in RC beams. The nonlinearities of materials and the practical interaction of components were considered in the proposed model. Subsequently, the developed numerical model is validated with available experimental findings reported in the literature, which demonstrates the effective approach in assessing the hybrid system of ECC material and CFRP sheets in retrofitting the RC beams.

2. Specimen dimensions and material properties

2.1. Specimen dimensions

Test results of the strengthened RC beam reported by Zhang et al [14] is used as a sort of reference data to construct the finite element model. Five beams were fabricated, including one unstrengthened beam, one beam with only strengthened ECC layer at the bottom (Figure 1) and three beams with ECC layer and CFRP sheets applied at the bottom, named as RCS-X beams with X denotes 1, 2, or 3 CFRP sheets (Figure 2). For example, RCS-1 represents that the RC beam was strengthened with ECC

and one layer of CFRP sheet. To enhance the cohesive force between the strengthened layer and RC beam, a CFRP sheet hoop was used at the end of the beam. The details of beams shown in Table 1.

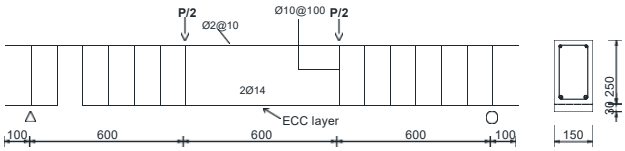

Figure 1. *Dimensions and configurations of RCS-0 beam*

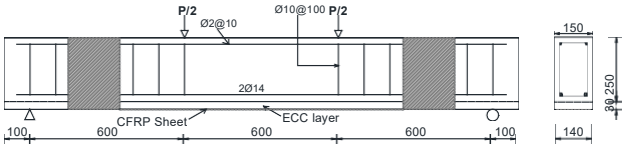

Figure 2. *Dimensions and configurations of RCS-X beam*

Table 1. *The design of beams [14]*

No.	Name of beams	ECC material layer (mm)	CFRP sheet (mm)	Layer of CFRP
1	RC	_	_	_
2	RCS-0	30 mm	_	_
3	RCS-1	30 mm	0.167 mm	1
4	RCS-2	30 mm	0.167 mm	2
5	RCS-3	30 mm	0.167 mm	3

The ECC layer has dimensions of 2000 mm (length) × 30 mm (height) × 150 mm (width). It is applied directly beneath the beams for strengthening. The CFRP sheet was used as the strengthened layer with dimensions of 1600 mm (length) × 0.167 mm (thickness) × 140 mm (width).

2.2. Material properties

The average compressive strength of concrete after 28 days was determined to be $f_c = 46.3$ Mpa in [14]. The ribbed steel bar with a diameter of 14 mm was used in the tensile zone while the compressive zone arranged with 10 mm diameter bars, and 10 mm diameter reinforcements was used for shear load resistance. To guarantee the flexural failure of the RC beam, the stirrups were arranged in the shear span. The steel bar parameters are obtained from reference [14] and shown in Table 2. The average compressive strength of ECC after 28 days was determined to be $f_{ecc} = 43.5$ MPa. The material properties of the CFRP sheet are shown in Table 3 [14].

Table 2. *Parameters of reinforcement*

Elastic modulus (GPa)	Yield strength (MPa)	Yield strain (mm/mm)	Tensile strength (MPa)	Tensile strain (mm/mm)
210	445	0.21	615	11.4

Table 3. *Parameters of CFRP sheets*

Elastic modulus (GPa)	Tensile strength (MPa)	Tensile strain (mm/mm)
270	3850	1.5

3. Finite element (FE) model development

The implementation steps in ABAQUS are presented in Figure 3.

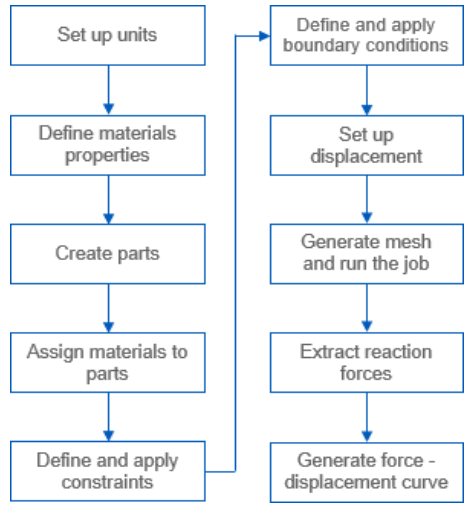

Figure 3. *Flowchart of the model development process in ABAQUS/CAE*

3.1. Element types, mesh sizes and constitutive models

3.1.1. Concrete

Solid element with reduced integration (C3D8R) with mesh size of 30 mm is used to simulate the concrete in RC part (Figure 4) of the beams. For modelling the behaviour of concrete in ABAQUS, Concrete Damage Plasticity (CDP) model is employed and the values are shown in Table 4.

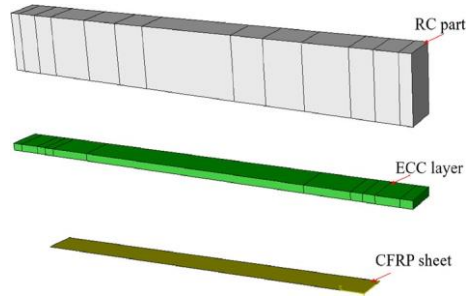

Figure 4. *Different components of strengthened RC beam modelled in ABAQUS*

Table 2. *The CDP parameters*

Poison's ratio	Dilation Angle (°)	Eccentricity	fb0/fc0	K	Viscosity Parameter
0.2	30	0.1	1.16	0.6667	0.0001

The compression constitutive of concrete is modeled using the following equation suggested in [15] and depicted in Figure 5:

$$\sigma_c = \frac{f'_c \gamma (\varepsilon_c / \varepsilon'_c)}{\gamma - 1 + (\varepsilon_c / \varepsilon')^{\gamma}} \quad (1)$$

where: σ_c is the concrete compressive stress, f'_c is concrete the compressive strength tested using cylinder, ε_c is the concrete compressive strain, ε'_c is the strain at the compressive strength. The γ value is calculated as follows:

$$\gamma = \left(\frac{f'_c}{32.4}\right)^3 + 1.55 \quad (2)$$

The tensile stress–strain model of concrete is shown in Figure 6 and illustrated in Eq. 3:

$$\sigma_t = f_t e^{-\left(\frac{\varepsilon-\varepsilon_{cr}}{0.00035}\right)^{0.85}} \quad (3)$$

where: ε_{cr} is the strain when the concrete reaches the tensile strength f_t.

The elastic modulus of concrete is approximately calculated as follows according to ACI 318 [16]:

$$E_0 = 4700\sqrt{f'_c} \quad (4)$$

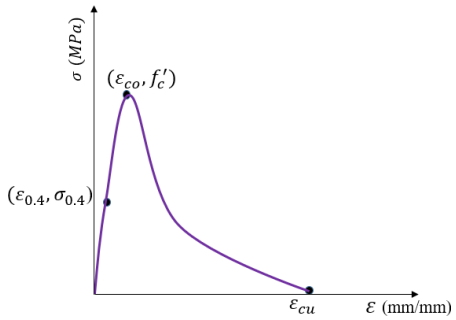

Figure 5. *Compressive stress-strain model of concrete*

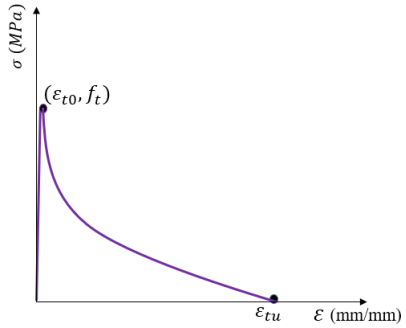

Figure 6. *Tensile stress-strain model of concrete*

3.1.2. Reinforcement

The steel reinforcement is simulated using two-node truss element (T3D2) with mesh size of 50 mm. Constitutive model of reinforcement is represented by a bilinear curve, as illustrated in Figure 7.

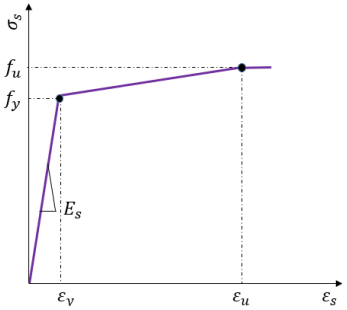

Figure 7. *Bilinear stress-strain curve of reinforcement*

3.1.3. ECC material

Similar to concrete, a solid element with reduced integration (C3D8R) with 30 mm mesh size is used to simulate ECC layer (Figure 3). The compressive stress-strain model of ECC shown in Figure 8 [17] is expressed as follows:

$$\sigma = \begin{cases} E_0\varepsilon & (0 < \varepsilon < \varepsilon_{0.4}) \\ E_0\varepsilon(1-\alpha) & (\varepsilon_{0.4} < \varepsilon < \varepsilon_0) \end{cases} \quad (5)$$

where: E_0 is the elastic modulus. ECC is considered to be linear elastic before reaching strain at 40% of compressive strength ($\varepsilon_{0.4}$). Beyond that, the reduction coefficient of elastic modulus α is applied:

$$\alpha = a\frac{\varepsilon E_0}{f'_{cr}} - b \quad (6)$$

where: f'_{cr} is the compressive strength of ECC, a and b are coefficients and are taken as 0.46 and 0.33, respectively.

The tensile behavior of ECC [17] is shown in Figure 9 and is expressed in the following equation:

$$\sigma_t = \begin{cases} E_0\varepsilon & (0 < \varepsilon < \varepsilon_{t0}) \\ \sigma_{t0} + (\sigma_{tp} - \sigma_{t0})\left(\frac{\varepsilon - \varepsilon_{t0}}{\varepsilon_{tp} - \varepsilon_{t0}}\right) & (\varepsilon_{t0} < \varepsilon < \varepsilon_{tp}) \\ \sigma_{tp}\left(\frac{\varepsilon - \varepsilon_{tp}}{\varepsilon_{tu} - \varepsilon_{tp}}\right) & (\varepsilon_{tp} < \varepsilon < \varepsilon_{tu}) \end{cases} \quad (7)$$

where: σ_{t0} and ε_{t0} are the stress and strain at the first crack, σ_{tp} and ε_{tp} are the tensile stress and strain, ε_{tu} is the strain at the point of failure.

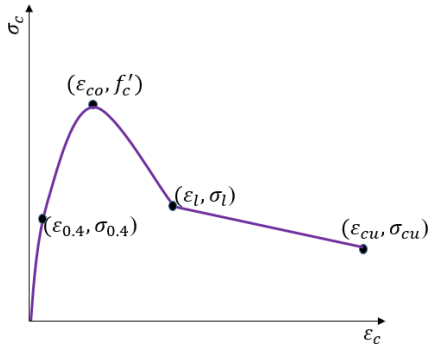

Figure 8. *Compressive stress-strain tensile model of ECC*

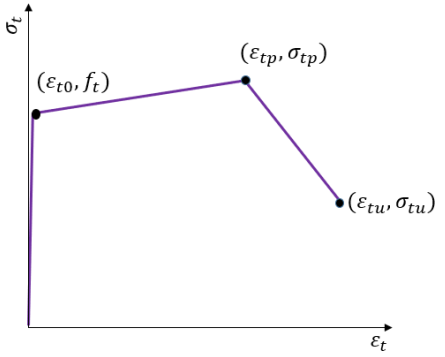

Figure 9. *Tensile stress-strain model of ECC*

3.1.4. CFRP sheets

The CFRP sheets and CFRP hoops are simulated using four-node shell elements (S4R) with mesh size of 30 mm. The elastic behavior of CFRP sheets is shown in Table 5, in which E1 and E2 represent the elastic modulus in the direction of CFRP fiber and perpendicular direction, respectively.

Table 5. *Elastic behavior of CFRP sheets*

E1 (MPa)	E2 (MPa)	Nu12	G12 (MPa)	G13 (MPa)	G23 (MPa)
270000	50000	0.28	90000	90000	80000

Table 6. *Coefficients of Hashin model*

Long. Tensile Strength (MPa)	Long. Compressive Strength (MPa)	Trans. Tensile Strength (MPa)	Trans. Compressive Strength (MPa)	Long. Shear Strength (MPa)	Trans. Shear Strength (MPa)
3850	3000	180	80	110	60

Table 7. *Value of parameters for interface of ECC and beams*

Friction Coefficient, μ	K_n, K_s, K_t (N/mm³)	Damage		
		$\delta_n^0, \delta_s^0, \delta_t^0$ (mm)	$\delta_m^{max} - \delta_m^0$ (mm)	Viscosity Coefficient
0.7	40	0.03	0.001	0.001

Table 8. *Value of parameters for interface of CFRP and beams*

Friction Coefficient, μ	K_n (N/mm³)	K_s (N/mm³)	K_t (N/mm³)
1.5	1000	500	500

Material property representation of CFRP sheets has two phases. The first is the representation of elastic behavior, which requires defining the two values of the modulus of elasticity, Poisson ratio, as well as the shear modulus, as tabulated in Table 5. Additionally, in order to represent the second phase (failure behavior), the Hashin damage model is used, as indicated in Table 6, in which the values of defined tensile strength, compressive strength, and shear strength required to construct the Hashin model, are shown.

3.2. Interactions

To ensure optimal modeling conditions, the loading plates and the supports are modeled as rigid materials. The interaction between the RC beam and two loading plates, as well as the two support plates, is defined using tie constraint. On the other hand, the interaction between concrete beams and reinforcement is modelled using embedded region available in ABAQUS.

The ECC layer at the bottom of the beam is bonded to the RC part using an impregnating adhesive. In the numerical model, surface-to-surface contact is inserted between ECC and concrete interfaces to model the interfacial bond-slip and cohesive behaviors. The damage initiation, evolution and stabilization parameters employed to define interfacial bond behavior between concrete and ECC are listed in Table 7 [18].

For RCS-X beams, the CFRP sheet was bonded to the concrete beam using an epoxy resin. To simulate the bond with possible slip or debonding between CFRP and concrete, a surface-to-surface contact is used with the behavior parameters as shown in Table 8 [19].

3.3. Boundary conditions

As illustrated in the test setup reported in [14], the simple beams were subjected to a four-point bending test. To simulate the boundary conditions of the beams, roller and pinned supports are used in the FE model. The displacement is applied on the loading surfaces to represent the load applied to the beams, as depicted in Figure 10.

4. Results and Discussion

The results obtained from the developed FE model are obtained and compared with the experimental findings in terms of failure mode, load-carrying capacity and displacement.

The typical failure mode found in both the experiment and FE model is the debonding of the ECC layer and RC part, which is shown in Figure 11. In most cases, CFRP remained intact at the failure (Figure 12). Crack distribution of RCS-3 beam obtained from the FE model compared to the test of [14] and shown in Figure 13. From Figures 11 - 13, it is indicated that the test and the FE model agree well with each other in terms of failure mode and crack distribution.

In terms of failure mode, debonding failure occurred at the interface between concrete and ECC which can be observed in both the test of Zhang et al. [14] and the FE model (Figure 11). It is worth noting that CFRP sheets remained intact and the strain value was quite small in the FE model (Figure 12) as well as observed in [14], due to the debonding failure occurred. Regarding crack distribution, flexural cracks are distributed mostly in the bending zone, which can be seen in the test [14] and the FE model (Figure 13).

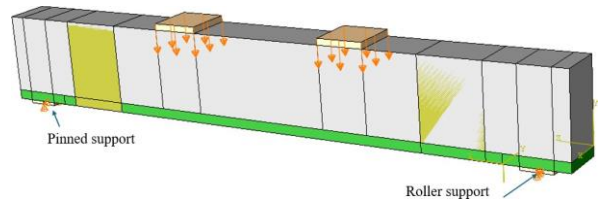

Figure 10. *Boundary conditions of the FE model*

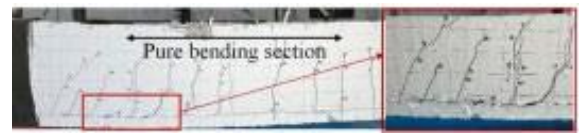

a) Experiment [14]

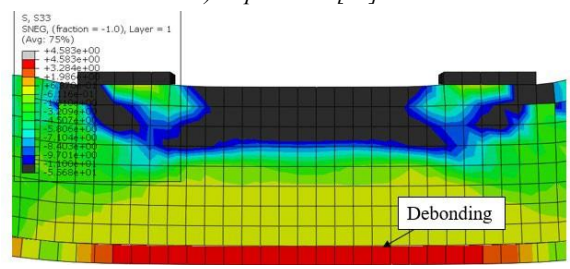

b) FE model

Figure 11. *Failure mode of RCS-3 beam*

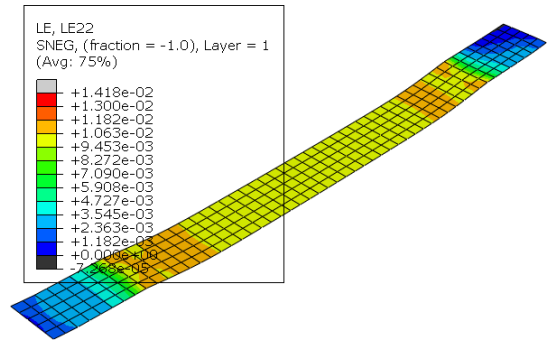

Figure 12. *Tensile strain in CFRP sheet at failure of RCS-3 beam obtained from the developed FE model*

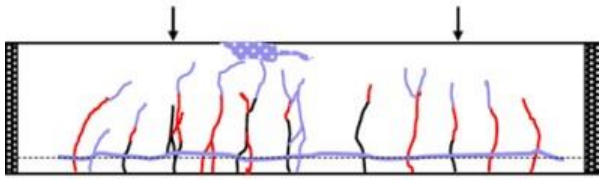

a) Experiment [14]

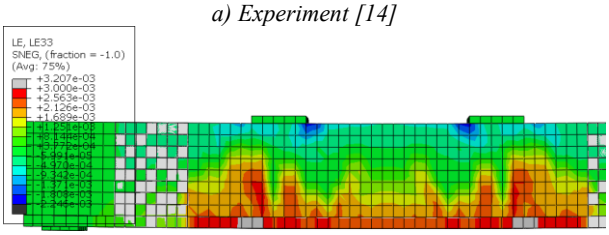

b) FE model

Figure 13. *Crack distribution of RCS-3 beam*

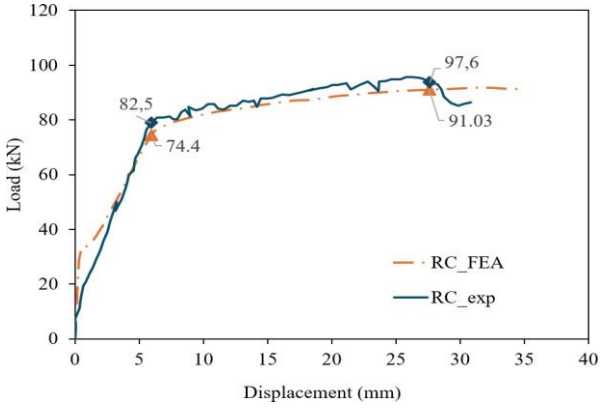

Figure 14. *Load-displacement relationship of RC beam*

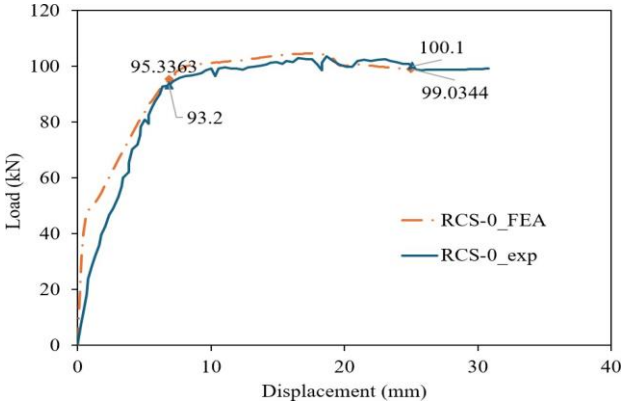

Figure 15. *Load-displacement relationship of RCS-0 beam*

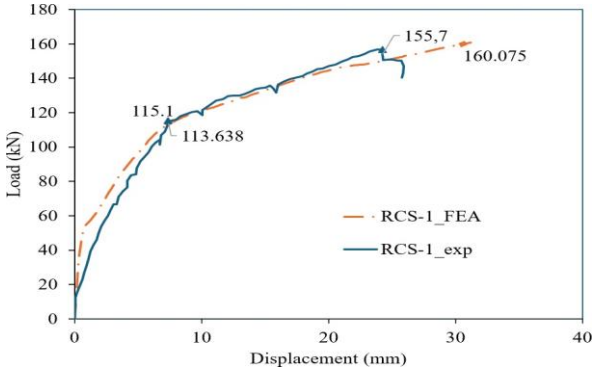

Figure 16. *Load-displacement relationship of RCS-1 beam*

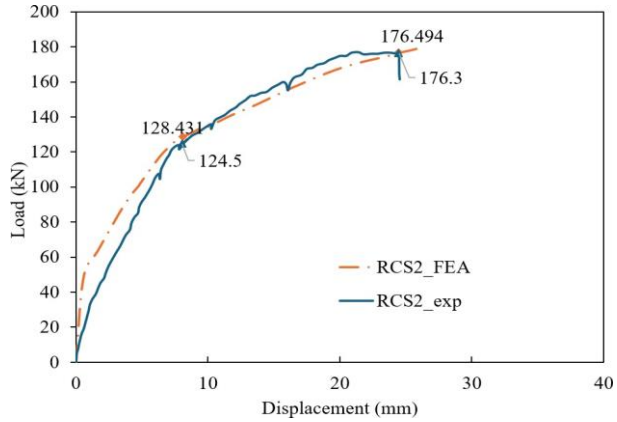

Figure 17. *Load–displacement relationship of RCS-2 beam*

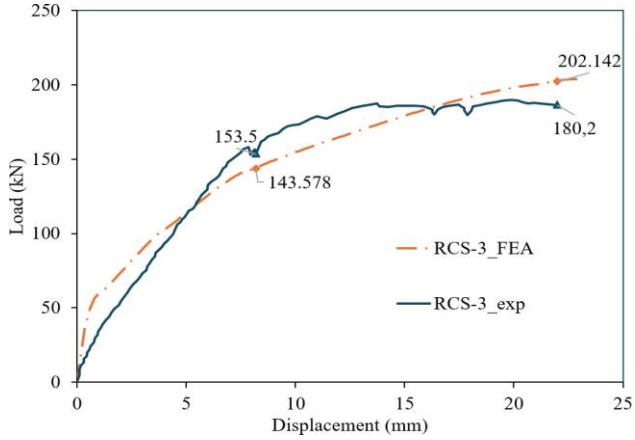

Figure 18. *Load–displacement relationship of RCS-3 beam*

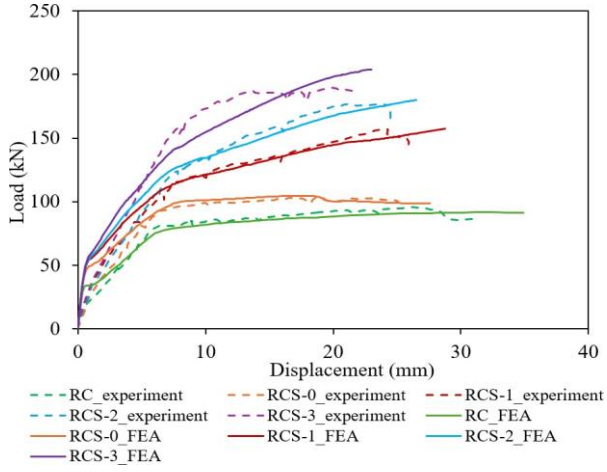

Figure 19. *Summary of load-displacement relationship*

Table 9. *Compare models and experimental results*

Beams	Yield load (kN)		Flexural load (kN)		Deviation (%)	
	Exp	FEA	Exp	FEA	Yield load	Flexural load
RC	82.5	74.4	97.6	91.03	10.89 %	7.22 %
RCS-0	95.33	93.2	100.1	99.03	2.29 %	1.08 %
RCS-1	115.1	113.63	155.7	160.1	1.29 %	2.75 %
RCS-2	128.43	124.5	176.3	176.5	3.16 %	0.11 %
RCS-3	153.5	143.6	180.2	202.1	6.89 %	10.84 %
Average					4.9 %	4.4 %

The load-displacement curves of the beams extracted from the FE model and experimental program [14] are indicated in Figures 13 – 18. From these figures, it is seen that the test and FE modelling results are in good agreement not only in the yielding load but also in the flexural load. By collecting the data from the above figures, the results obtained from the test [14] and FE model of the beams are summarized in Table 9. From Figures 14 -19 as well as Table 9, it can be observed that the load-displacement behaviour obtained from the numerical simulation closely agrees with the experimental data for all beam types, with the average deviations being only 4.9% and 4.4% for the yield load and flexural load, respectively.

5. Conclusions

This study has developed and validated the accuracy of the finite element model in simulating the RC beams strengthened using ECC layer and CFRP sheets against experimental studies published in the literature. The simulation results exhibited a high correlation with experimental data, not only in terms of failure mode but also the flexural strength, with an average deviation of only 4.4%. This confirms the feasibility of the validated numerical modeling proposed in this study in predicting the behavior of RC beams strengthened with ECC layer and CFRP sheets, which enables the assessment of the strengthening efficiency of RC beams without the need for physical testing. However, the paper has barely presented the development of the numerical model in predicting the flexural behaviour of ECC-CFRP strengthening RC beams. In future works, the effect of key parameters, such as the thickness of the ECC layer, the quantity of CFRP layers, the arrangement of the CFRP layer, etc., needs to be thoroughly studied.

Acknowledgment: This work was supported by Murata Fund and The University of Danang - University of Science and Technology, code number of Project: T2024-02-10MSF.

REFERENCES

[1] R. Vali, "Water table effects on the behaviors of the reinforced marine soil-footing system", *Journal of Human, Earth, and Future,* vol. 2, no. 3, pp. 296-305, 2021. http://dx.doi.org/10. 28991/HEF-2021-02-03-09.

[2] V. G. Konstantinos, and E. D. Stephanos, "Concrete jacket construction detail effectiveness when strengthening RC columns", *Construction and Building Materials*, vol. 22, no. 3, pp. 264-276, 2008. https://doi.org/10.1016/j.conbuildmat.2006.08.019

[3] G. Ruano, F. Isla, R. I. Pedraza, D. Sfer, and B. Luccioni, "Shear retrofitting of reinforced concrete beams with steel fiber reinforced concrete", *Construction and Building Materials*, vol. 54, pp. 646-658, 2014. https://doi.org/10.1016/j.conbuildmat.2013.12.092

[4] P. Nagaprasad, D. R. Sahoo, and D. C. Rai, "Seismic strengthening of RC columns using external steel cage", *Earthquake Engineering & Structural Dynamics,* vol. 38, no. 14, pp.1563-1586, 2009. https://doi.org/10.1002/eqe.917

[5] E. Oller, M. Pujol, and A. Marí, "Contribution of externally bonded FRP shear reinforcement to the shear strength of RC beams", *Composites Part B: Engineering,* vol. 164, pp. 235-248, 2019. https://doi.org/10.1016/j.compositesb.2018.11.065

[6] H. B. Huang, W. Zhang, Z. G. Sun, and D. S Wang, "Probabilistic models for predicting bond strength of externally bonded FRP-to-concrete joints based on Bayesian inference", *Construction and Building Materials,* vol. 329, pp. 127194, 2022. https://doi.org/10.1016/j.conbuildmat.2022.127194

[7] C. K. Y. Leung, "FRP debonding from a concrete substrate: Some recent findings against conventional belief", *Cement and Concrete Composites*, vol. 28, no. 8, pp. 742-748, 2006. https://doi.org/10.1016/j.cemconcomp.2006.05.015

[8] A. G. Razaqpur, R. Cameron, and A. A. B. Mostafa, "Strengthening of RC beams with externally bonded and anchored thick CFRP laminate", *Composite Structures*, vol. 233, pp. 111574, 2020. https://doi.org/10.1016/j.compstruct.2019.111574

[9] Y. Zheng, L. F. Zhang, and L. P. Xia, "Investigation of the behaviour of flexible and ductile ECC link slab reinforced with FRP", *Construction and Building Materials*, vol. 166, pp. 694-711, 2018. https://doi.org/10.1016/j.conbuildmat.2018.01.188

[10] H. Liu, Q. Zhang, C. Gu, H. Su, and V. Li, "Influence of microcrack self-healing behavior on the permeability of Engineered Cementitious Composites", *Cement and Concrete Composites*, vol. 82, pp. 14-22, 2017. https://doi.org/10.1016/j.cemconcomp.2017.04.004

[11] C. Wu, and V. C. Li, "CFRP-ECC hybrid for strengthening of the concrete structures", *Composite Structures*, vol. 178, pp. 372-382, 2017. https://doi.org/10.1016/j.compstruct.2017.07.034

[12] Y. Zhou, L. Sui, X. Huang, M. Guo, M. Luo, B. Hu, and C. Chen, "Enhancing the EB-FRP strengthening effectiveness by incorporating a cracking-control layer of ECC with different thicknesses", *Construction and Building Materials*, vol. 286, pp. 122975, 2021. https://doi.org/10.1016/j.conbuildmat.2021.122975Get rights and content

[13] B. Hu, Y. Zhou, F. Xing, L. Sui, and M. Luo, "Experimental and theoretical investigation on the hybrid CFRP-ECC flexural strengthening of RC beams with corroded longitudinal reinforcement", *Engineering Structures*, vol. 200, pp. 109717, 2019. https://doi.org/10.1016/j.engstruct.2019.109717

[14] P. Zhang, Y. Su, J. Shang, Z. Xu, T. Hao, C. Wu, and S. A. Sheikh, "Flexural behavior of RC beams strengthened with CFRP sheets and ECC material", *Structures*, vol. 61, pp. 106015, 2024. https://doi.org/10.1016/j.istruc.2024.106015

[15] D. J. Carreira, and K. H. Chu, "Stress-strain relationship for plain concrete in compression", *ACI Journal*, vol. 82, no. 6, pp. 797-804, 1985.

[16] *Building code requirements for structural concrete*, ACI 318-11, American Concrete Institute, 2011.

[17] D. Meng, T. Huang, Y. X. Zhang, and C. K. Lee, "Mechanical behaviour of a polyvinyl alcohol fibre reinforced engineered cementitious composite (PVA-ECC) using local ingredients", *Construction and Building Materials*, vol. 141, pp. 259-270, 2017. https://doi.org/10.1016/j.conbuildmat.2017.02.158

[18] M. Qasim, C.K. Lee, and Y.X. Zhang, "Flexural strengthening of reinforced concrete beams using hybrid fibre reinforced engineered cementitious composite", *Engineering Structures*, vol. 284, pp. 115992, 2023. https://doi.org/10.1016/j.engstruct.2023.115992

[19] W. Mansour, W. Li, P. Wang, and M. Badawi, "Experimental and numerical evaluations of the shear performance of recycled aggregate RC beams strengthened using CFRP sheets", *Engineering Structures*, vol. 301, pp. 117368, 2024. https://doi.org/10.1016/j.engstruct.2023.117368.